

## Original Research

# Targeting histone deacetylase SIRT1 selectively eradicates EGFR TKI-resistant cancer stem cells via regulation of mitochondrial oxidative phosphorylation in lung adenocarcinoma



Jiangtao Sun<sup>a,c,1</sup>; Guifang Li<sup>a,c,1</sup>; Yiwen Liu<sup>a</sup>;  
Mingyang Ma<sup>a,c</sup>; Kaifang Song<sup>a</sup>; Huaxu Li<sup>d</sup>; Daxing  
Zhu<sup>b</sup>; XiaoJun Tang<sup>b</sup>; Jinyu Kong<sup>c</sup>;  
Xiang Yuan<sup>a,c</sup>

<sup>a</sup>Department of Pulmonary Tumor Surgery, Cancer Hospital, The First Affiliated Hospital, College of Clinical Medicine, Medical College of Henan University of Science and Technology, Luoyang 471003, China; <sup>b</sup>The Lung Cancer Center, West China Hospital of Sichuan University, Chengdu, Sichuan 610000, China; <sup>c</sup>Henan Key Laboratory of Cancer Epigenetics, Cancer Hospital, The First Affiliated Hospital, College of Clinical Medicine, Medical College of Henan University of Science and Technology, Luoyang 471003, China; <sup>d</sup>Queen Mary College, Medical College of Nanchang University, Nanchang 330006, China

## Abstract

Lung adenocarcinoma (LAD) is a human malignancy successfully treated with the tyrosine kinase inhibitor (TKI) gefitinib; however, the enrichment of therapy resistant cancer stem cells (CSCs) in such patients is assumed to be a source of treatment failure. Evaluation of LAD cell populations treated with the TKI inhibitor gefitinib identified unique aspects of a subpopulation of tumor cells exhibiting stemlike properties and mitochondriaspecific metabolic features along with their reliance on sirtuin 1 (SIRT1) for survival advantage. This addiction to bioenergetic metabolism in LAD treated with EGFRtargeted therapy suggests that mitochondrial targeting should be synthetically lethal using established cytotoxic therapies. Accordingly, loss of the phenotype present in resistant CSC clones either by targeting the energy metabolism with tigecycline, a mitochondrial DNAtranslation inhibitor, or tenovin6 (TV6), a SIRT1 inhibitor, inhibited their dependency on mitochondrial oxidative phosphorylation (mtOXPHOS) and sensitized them for a more pronounced and longlasting TKI therapeutic effect. The results specifically demonstrated that combined therapy with TV6 and gefitinib resulted in tumor regression in xenograft mouse models, whereas administration of a single agent showed no such efficacy. Importantly, combined treatment with TV6 also decreased the effective dose of gefitinib necessary for treatment response. Clinical analysis demonstrated that highprofile SIRT1 and mtOXPHOS proteins were associated with recurrence and poor prognosis in LAD patients. These observations support the CSC hypothesis for cancer relapse and advocate use of mitochondriatargeting inhibitors as part of combinatorial therapy in a variety of clinical settings, as well as for reducing firstline TKI dosage in LAD patients.

*Neoplastic* (2019) 22 33–46

## Introduction

Targeting oncogenedriven signaling pathways is a clinically validated approach for treating several devastating diseases. Gefitinib is a selective inhibitor of epidermal growth factor receptor (EGFR) mutation and constitutes a paradigm shift in lung adenocarcinoma (LAD) therapy [1].

Received 5 October 2019; accepted 21 October 2019  
© 2019 The Authors. Published by Elsevier Inc. on behalf of Neoplasia Press, Inc. This is an open access article under the CC BY-NC-ND license (<http://creativecommons.org/licenses/by-nc-nd/4.0/>).

**Abbreviations:** LAD, Lung adenocarcinoma, CSCs, Cancer stem cells, TKI, tyrosine kinase inhibitor, IC50, half maximal inhibitory concentration, mtOXPHOS, mitochondrial oxidative phosphorylation

Corresponding author at: Department of Pulmonary Tumor Surgery, Cancer Hospital, The First Affiliated Hospital, College of Clinical Medicine, Medical College of Henan University of Science and Technology, 24 Jinghua Road, Jianxi District, Luoyang, Henan 471003, China.

e-mail address: [yuanxiangdrive@163.com](mailto:yuanxiangdrive@163.com) (X. Yuan).

<sup>1</sup> Co-first authors.

Unfortunately, acquired resistance and early relapses, which unavoidably occur, represent a major limitation to clinical responses [2]. To explain this phenomenon, the cancer stem cell (CSC) hypothesis suggests that tumors contain a small number of tumorforming and selfrenewing stem cells that are less responsive to gefitinib and other tyrosine kinase inhibitors (TKIs) and constitute a critical target population for acquisition of drug resistance [3–5]. Therefore, strategies to prevent the reemergence of CSCs have been devised to augment the impact of anticancer therapy.

The comprehensive evidence for bioenergetic metabolism reprogramming of tumor cells has received increased attention during the previous decade [6]. Studies demonstrated mitochondriaspecific oxidative features as a specific vulnerability of cells exhibiting therapy selective quiescence (TSQ), which when exploited, should be amendable to established cytotoxic interventions and provide the basis for developing more effective therapies to combat lethal disease [7,8]. Minimally, this would apply to lymphomas undergoing TSQ in response to cytotoxic therapy [7], minimal residual leukemia resistant to TKIs [9], slowcycling melanoma cells selected for a JARID1B<sup>high</sup> phenotype by cytotoxic agents [10], BRAF-mutant melanomas escaping therapy with BRAF inhibitors [11], and a subpopulation of dormant pancreatic cancer cells surviving KRAS oncogene ablation [12]. These examples strongly suggest that reliance on mitochondrial metabolism might represent a measure of druggable susceptibility by multidrugresistant cancers. Comprehensive evidence for a mitochondrial role in LAD cells exhibiting TSQ and the genes responsible for this process is inconclusive [13,14].

The nicotinamide adenine dinucleotide (NAD)dependent histone deacetylase sirtuin 1 (SIRT1) is a nuclear protein expressed in almost all cell types and that plays a major role in stemness maintenance and TKI resistance, as well as being involved in modulating gene expression, aging, development, and many metabolic and stressresponse pathways [15–17].

The aim of this study was to elucidate the mechanism(s) involved in cellular perturbations accompanying acquired gefitinib resistance in order to provide new therapeutics to target TSQ cells and achieve therapy free remission in LAD patients. Additionally, we evaluated new possibilities of the synergism of tenovin6 (TV6) [18–20], a smallmolecule compound that inhibits SIRT1, with reduced doses of conventional cytotoxic therapies currently ineffective as monotherapies for future application in clinical settings to treat LAD.

## Materials & Methods

### Study participants

From 2007 to 2014, a multicenter research of lung adenocarcinoma drew subjects primarily from the Taihang Mountain region of Henan provinces, including the First Affiliated Hospital of Henan University of Science and Technology (HUST; Luoyang, Henan, China) and Anyang Tumor Hospital (ATH; Anyang, Henan, China). Tumor specimens containing the EGFR exon 19 deletion or L858R sensitive mutation were obtained with informed consent in accordance with the institutional review boards at HUST and ATH. Treatment nave patients had a core biopsy from the primary lung tumor or surgical resection; and patients that relapsed under Gefitinib had a fine needle biopsy from a primary tumor or metastasis. All patients had an initial partial response, followed by disease progression after 120 days of Gefitinib therapy. The presence of EGFR mutations in each specimen was determined by PCRbased direct sequencing. No restrictions regarding age, sex, or disease stage were set. Patients who had received any preoperative radio, chemo or immune therapy before recruitment were excluded. Each specimen was sufficient to be cut into pieces and treated differently for various uses, put in liquid nitrogen to extract RNA for RNA sequencing, or fixed in 10% formaldehyde for making paraffin embedded blocks. Additional fresh LAD specimens

were collected, for isolation and identification of ALDH1<sup>bri+</sup> cells or generation of patientderived xenografts (PDXs).

### High-throughput RNA sequencing and data analysis

The constructed libraries were sequenced using an Illumina HiSeq 2500 system (Illumina). Lowquality reads, short reads, rRNAs, and reads containing primer/adaptor contamination were removed. The remaining highquality reads were mapped to a reference genome (mm10) with two mismatches using Tophat (v.2.0.9; <https://ccb.jhu.edu/software/tophat/index.shtml>), and results were expressed as fragments per kilobase of transcript per million mapped reads (FPKM). The genes in the libraries were produced using the Cufflinks tool (v.2.1.1; <http://cole-trapnell-lab.github.io/cufflinks/>) according to the reference annotation set (mm10). Fold changes for the genes in different samples were estimated based on their FPKM values, and the significance threshold was determined according to the false discovery rate (FDR). In this study, a differentially expressed gene was defined as a gene whose expression changed more than twofold among the different samples with an FDR 0.05.

### Gene set enrichment analysis (GSEA)

Ranked lists of differentially expressed genes (fold change 1.5;  $t$  test  $p$  0.05) were assessed through the GSEA desktop application using the GSEAPreranked tool (<http://software.broadinstitute.org/cancer/software/genepattern/modules/docs/GSEAPreranked/1>). Curated gene sets (C2) from the Molecular Signatures Database (v5.0; <http://software.broadinstitute.org/gsea/msigdb/index.jsp>) were interrogated, and after filtering out genes not in the expression dataset, gene sets of <15 genes or >3000 genes were excluded from analysis. GSEA was run using 1000 geneset permutations to generate FDRs. Default settings were used for normalizing the enrichment scores (NES).

### In vivo studies

We used a patientderived xenograft (PDX) model, in which 1 to 2mm fragments of tumors from postrelapsed LAD patients under gefitinib treatment were orthotopically implanted into the mammary fat pad of NOD/SCID interleukin2 receptor chaindeficient (NSG) mice. After implantation, the mice were randomly divided into four different groups ( $n = 10/\text{group}$ ) and treated 14 days later for a period of 3 weeks by intraperitoneal (i.p.) injection with gefitinib (100 mg/kg, daily), TV6 (50 mg/kg, daily), both drugs combined, and vehicle only twice daily. The animals dosed according to the appropriate scheme were monitored daily for up to 3 months, and the objective response rate and survival were recorded. An additional cohort of mice ( $n = 3/\text{group}$ ) was included to conduct mechanistic studies. In this cohort, the mice were sacrificed on day 40 postdrug administration, and residual tumors were surgically removed before terminal escape [tumor with partial response (PR); TV6 therapy] or complete remission [tumor with complete response (CR); combined therapy]. Resected tumors were processed for Aldefluor assay and flow cytometric analysis. Flow cytometry results related to the aldehyde dehydrogenase 1 (ALDH1)<sup>bri+</sup> fraction were determined, and a representative mouse from each treatment group in this separate cohort is shown. For studies on tumor rechallenge, 1 to 2mm diameter pieces of tumor taken from residual tumors surgically removed on day 25 postdrug administration were implanted into another cohort of NSG mice ( $n = 5/\text{group}$ ), and the engraftments were recorded. CR was defined as complete regression of the tumor without any recurrence. Primary and secondary challenge tumor growth was followed for up to 90 and 28 days, respectively. Tumor growth was monitored by caliper measurements, and tumor volume (TV) was calculated as follows:  $\text{TV} (\text{mm}^3) = 1/6 \times \text{length} \times \text{width}^2$ .

Treatment with gefitinib, TV6, and their combination was conducted twice daily due to toxicity to TV6 and deviation from design of the animal study. Mice suffering from progressive disease or those used for subsequent analysis were euthanized when TV was  $>2500 \text{ mm}^3$ . The health status and weight of the mice was monitored daily, and mice were humanely euthanized when moribund, as defined by weight loss exceeding 10% to 15%, lethargy, ruffled fur, and/or partial or hindlimb paralysis. At the end of the measurement, mice were sacrificed, venous blood was drawn from the orbit of the mice for confirmation of drug tolerability, and serum levels of liver, muscle, or cardiac enzymes were determined.

Sixto 8weekold male nude mice were implanted subcutaneously with a total of  $5 \times 10^6$  PC9 green fluorescent protein (GFP)<sup>+</sup> cells, administered luciferin i.p., and imaged by noninvasive bioluminescence imaging using an IVIS Lumina system (Caliper Life Sciences, Waltham, MA, USA), all of which developed tumors within 14 days (size:  $55 \text{ mm}^3$ ). For each experiment, mice were randomly distributed into equal groups ( $n = 10$  mice/group) that were either untreated or treated with i.p. injections twice daily with 25 mg/kg/day or 100 mg/kg/day gefitinib, 50 mg/kg/day TV6, or TV6based combined therapy involving low or highdose gefitinib for 21 consecutive days. The animals dosed appropriately were monitored daily for 3 months, and the objective response rate and survival were recorded. Animals were sacrificed because of progressive disease if TV was  $>2500 \text{ mm}^3$  before the next measurement. CR was defined as a complete regression of the tumor without any recurrence.

### Statistical analysis

Results are presented as the mean standard error of the mean (SEM) or standard deviation (SD). Predefined pairwise comparisons of treated group(s) with the control group for the indicated time points were conducted. Kaplan–Meier survival analysis and multivariate Cox regression were performed using the R survival package (<https://cran.r-project.org/web/packages/survival/index.html>) and replotted using Graphpad Prism software (v.6.00; GraphPad Software, La Jolla, CA, USA). Log ratios, unpaired *t* test *p* values, and colorcoded heat maps were obtained using MATRIX. For comparisons involving progressively resistant cell lines, analyses were performed using the R package by fitting a linear regression model to geneexpression data against the logtransformed 50% inhibitory concentration (IC<sub>50</sub>) values as measures of drug response. Weibull parametric survival analysis was used to test the interaction effect of each combination of drugs in groups to determine synergy, additivity, less than additivity, or antagonism of survival. Unless indicated, the mean SEM is reported. A  $p < 0.05$  was considered significant.

## Results

### *Residual LAD that resist oncogene ablation exhibits CSC-like features and relies on SIRT1 for survival*

To establish in vitro models of LAD exhibiting EGFR TKI resistance, the LAD cell lines PC9 and HCC827 demonstrating exquisite TKI sensitivity were treated longterm ( $>6$  months) with increasing doses of gefitinib. This allowed development of a PC9 cell series of T5, T10, T15, and T20 resistant variants (Figure 1A) and HCC827 isogenic cell series of T4, T8, T16, and T20 resistant variants (Figure 1B) that showed progressive increases in resistance to gefitinib along with increasing treatment cycles, subsequently reaching increases in IC<sub>50</sub> for PC9 and HCC827 of T20 (Supplementary Figure S1A and B; Supplementary Table S1). Significantly, Aldefluor assay showed that the ALDH<sup>bri+</sup> cell populations constituted 31.06% of PC9 (Figure 1C and Supplementary Figure S1C) and

27.64% of HCC827 T20 cells (Figure 1D and Supplementary Figure S1D), with CSCs clearly enriched in drugresistant cell lines. Additionally, we conducted a sphereformation assay to examine the cellular functional features of stem celllike properties, finding that PC9 (Figure 1E and Supplementary Figure S1E) and HCC827 (Figure 1F and Supplementary Figure S1F) T20 cells acquired a higher ability to form spheres in suspension culture as compared with parental cells, indicating that T20 yielded small subpopulations of cancer cells capable of surviving highconcentration gefitinib exposure that kills the vast majority of cells, thereby reflecting phenotypic heterogeneity within the population.

To investigate the molecular changes accompanying the development of gefitinib resistance, we performed RNA sequencing of the entire progressively resistant isogenic PC9 and HCC827 cell series. We fitted a linear regression model to microarray data to systematically identify genes showing a progressive increase or decrease in expression consistent with increasing drug resistance as represented by the logtransformed IC<sub>50</sub> values across the entire series of progressed lines. We identified 1849 differentially expressed genes in the PC9 resistant series and 1910 genes in the HCC827 resistant series at an FDR of 0.1 (Supplementary Figure S1G). We then performed stringent filtering of the expression data to select genes exhibiting an overlap between the two progressively resistant cell line models. We further required these changes to occur in vivo in primary cancerous tissue from patients that relapsed under gefitinib treatment. We identified 93 upregulated and 75 downregulated genes that overlapped between the two resistant cell line series (Supplementary Figure S1H), whereas intersection with primary tumor profiles (Supplementary Figure S1I) identified 40 upregulated and 21 downregulated genes exhibiting differences in expression that were sustained in vivo (Supplementary Figure S1J). These 61 genes (Supplementary Figure S2A) formed our preclinical resistance signature.

Notably, among the topranked gene list that was upregulated in therapy exposed samples, we focused on the gene encoding SIRT1, a histone deacetylase involved in numerous processes, including selfrenewal and stemness maintenance and with particular functions in bioenergetic metabolism [21]. To test the survival dependency of resistant clones on SIRT1, we applied highly selective SIRT1 inhibitors TV6 and Selisistat (EX 527), findings that PC9 (Figure 1G) and HCC827 (Figure 1H) T20 cells showed higher sensitivity to these inhibitors as compared with parental cells. We then tested the pharmacologic sensitivity of ALDH1<sup>bri+</sup> cells derived from relapsed LAD patients to SIRT1 inhibitors, and found that the IC<sub>50</sub> values for this cell population after incubation were in a lower micromolar range than their ALDH1<sup>low</sup> counterparts (Figure 1I)

We then evaluated *SIRT1* expression levels in ALDH1<sup>bri+</sup> cells from eight relapsed LAD patients, resistant to gefitinib, and sorted by ALDH activity. ALDH1<sup>bri+</sup> cells displayed enhanced *SIRT1* expression as compared with that in ALDH1<sup>low</sup> counterparts (Supplementary Figure S2B). We then queried the entire progressively resistant PC9 (Supplementary Figure S2C) and HCC827 (Supplementary Figure S2D) series and found a consistent increase in *SIRT1* expression along with increasing resistance to TKI therapy.

To evaluate whether the hypersensitivity of TKIresistant cells was specific to SIRT family inhibitors or represented a general epigenetic susceptibility, we tested other compounds inhibiting JmjClysine demethylase (KDM), lysinespecific histone demethylase 1, histone methyltransferases, histone acetyltransferases, bromodomains, DNA methyltransferases, or histone deacetylases. We did not observe significant differences in IC<sub>50</sub> values for any of these drugs between parental cells and resistant variants (Supplementary Figure S3A). These results uncovered a specific, targetable vulnerability to SIRT inhibition that can be exploited to treat LADs exhibiting resistance to TKI therapy.

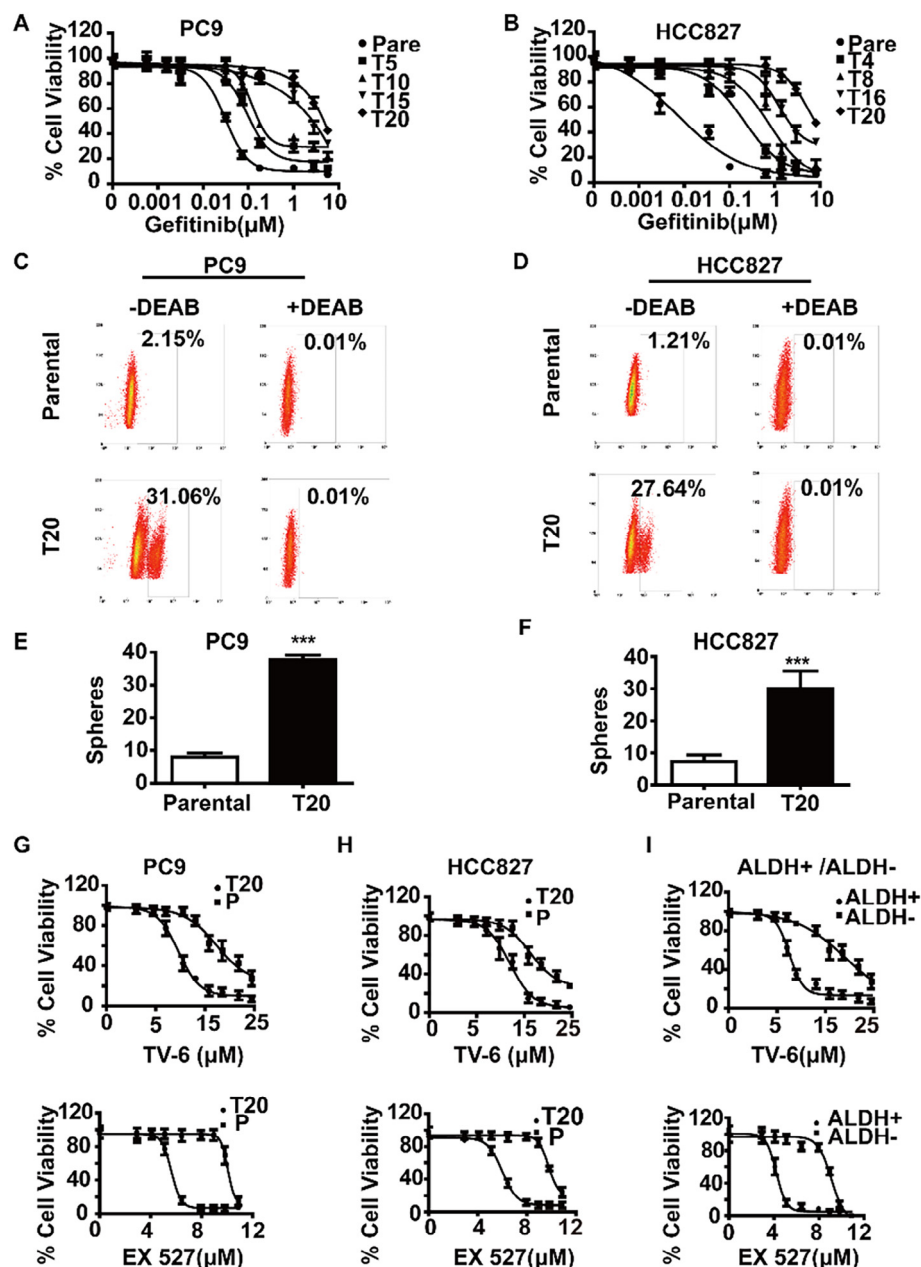


**Figure 1.** Residual LAD resistant to EGFR ablation exhibit CSC features and rely on SIRT1 for survival. A and B, Dose-response curves for PC9 (A) and HCC827 (B) cells after long-term treatment with gefitinib. P, parental cell line; T[n], resistant variant generated after n cycles of gefitinib. Values on the X-axis indicate gefitinib concentration (M). Each data point represents the mean SD of three replicates. C and D, Relative percentage of the ALDH<sup>br</sup> subpopulation of PC9 and HCC827 parental and T20 cells. E and F, Sphere-formation assay showing that PC9 and HCC827 T20 cells acquired an increased ability to form spheres in suspension culture relative to parental cells. G–I, PC9 (G), and HCC827 (H) T20 cells showed hypersensitivity to TV-6, as well as EX 527, as compared with parental cells. The result was the same as that for ALDH1<sup>br+</sup> cells (I) derived from relapsed LAD patients under gefitinib treatment. Each data point represents the mean SD of three replicates per drug dose.

#### *LAD treated with EGFR inhibitors are addicted to mitochondrial oxidative metabolism*

GSEA of the rankordered genes associated with drug sensitivity revealed prominent expression of genes governing hypoxia, autophagy, lysosome activity, and insulin secretion, as well as strong reliance on mitochondrial respiration for cellular energetics (Supplementary Table S2). Considering that malignant transformation involves cellular metabolic changes, which could in turn render the transformed cells susceptible to

specific assaults in a selective manner, we searched for such vulnerabilities in LAD.

Accordingly, in resistant PC9 and HCC827 T20 cells, the basal and maximal respiratory capacities of their CSC fractions were higher than those in their parental counterparts, suggesting activated mitochondrial (mt)OXPHOS (Figure 2A). Consistent with this result, mitochondrial membrane potentials (mtMPs) were also upregulated in PC9 and HCC827 T20 cells (Figure 2B). We then measured the levels of reactive oxygen species (ROS), which can be elevated through the activation of the

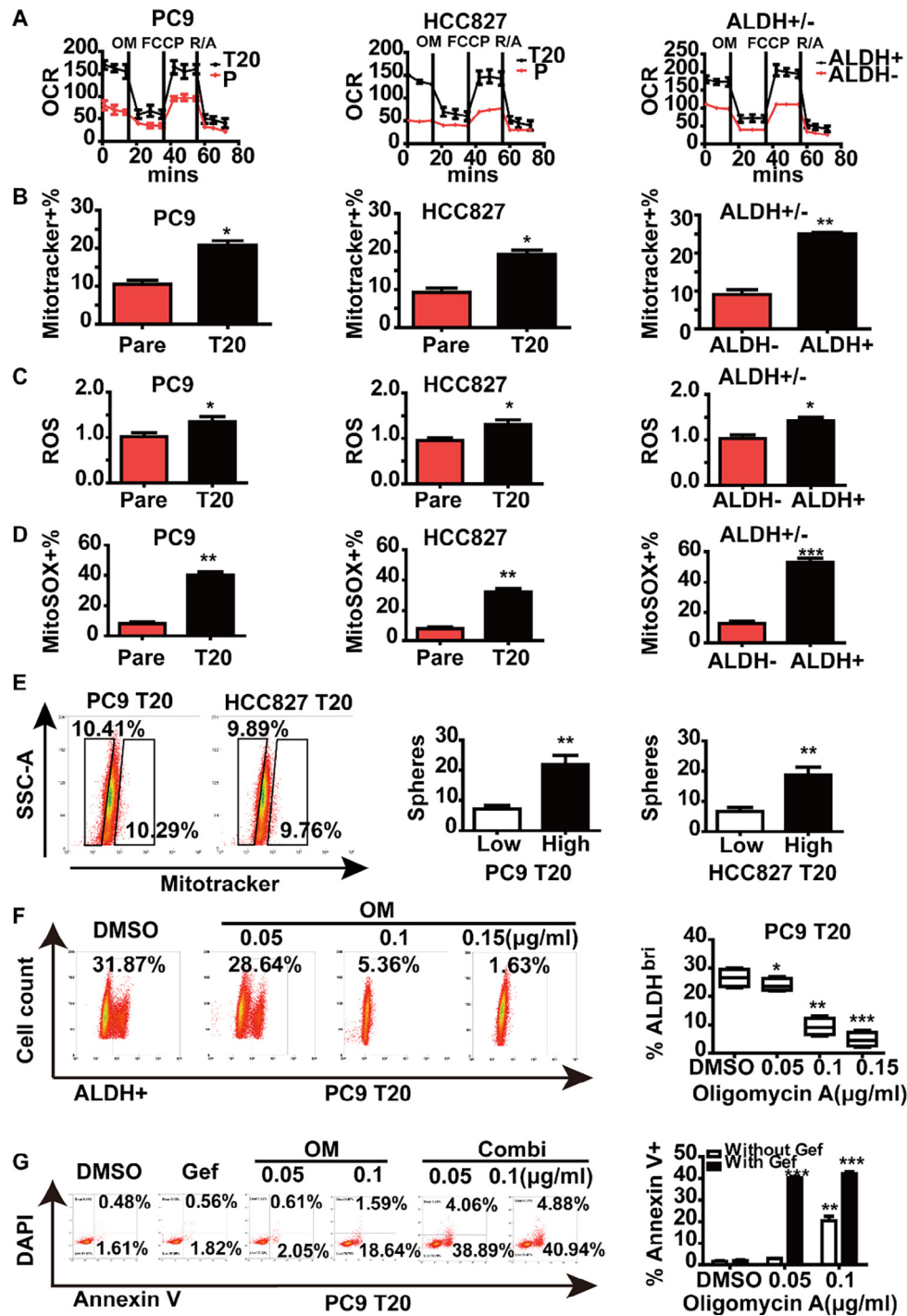


**Figure 2.** LAD CSCs exhibit an enhanced mitochondrial respiratory phenotype. A, OCRs were determined in a panel of LAD T20 and parental cells. B, LAD T20 and parental cells were stained with Mito Tracker Red CMX Ros and analyzed by flow cytometry. C, ROS levels were determined by ROS-Glo, as described in the STAR Methods. D, Cells were stained with Mito SOX Red and analyzed by flow cytometry. E, PC9 and HCC827 T20 cells were sorted by flow cytometry according to the intensity of Mito Tracker Red CMX Ros and then seeded for sphere assays. F, Relative percentage of the ALDH<sup>bri</sup> subpopulation of PC9 T20 cells under oligomycin A (OM) treatment at the indicated concentrations. G, PC9 T20 cells were treated with gefitinib (Gef) and/or OM at the indicated concentrations. Annexin V was used as a marker of cell death. A representative result from three independent flow cytometry experiments is shown. Data represent the mean SD.

electron transport chain in the mitochondria. Hydrogen peroxide (H<sub>2</sub>O<sub>2</sub>) and mitochondrial superoxide levels were elevated in PC9 and HCC827 T20 cells as compared with parental cells, which was in line with hyperactive mtOXPHOS (Figure 2C and D). Moreover, ALDH1<sup>bri</sup> cells

derived from residual LAD tumors following TKI therapy also exhibited elevated mtOXPHOS capacity, mtMPs, ROS levels, and mitochondrial superoxide levels as compared with their ALDH1<sup>low</sup> counterparts (Figure 2A–D). PC9 and HCC827 T20 cells were then sorted for high

versus low mtMPs by the intensity of MitoTracker Red CMX Ros and plated as spheres, revealing that sphere formation was markedly higher in cells with high mtMPs as compared with low mtMPs (Figure 2E).

To test the survival dependency of resistant clones on mtOXPHOS, we employed the mitochondriatargeted inhibitor tigecycline [22], which suppress mitochondrial DNA (mtDNA) translation, and oligomycin A [10], an ATP synthase inhibitor (Supplementary Figure S4A). PC9 (Supplementary Figure S4B) and HCC827 (Supplementary Figure S4C) T20 cells were severalfold hypersensitized to mitochondriatargeted inhibitors as compared with their corresponding parental cells. Moreover, targeting mitochondria with oligomycin A attenuated sphere formation (Supplementary Figure S4D) and the ALDH1<sup>bri+</sup> subpopulation (Figure 2F and Supplementary Figure S4E) by resistant CSC clones. Similarly, tigecycline reduced sphere formation (Supplementary Figure S4F) and the ALDH1<sup>bri+</sup> fraction (Supplementary Figure S4G). Even treatment with extremely low doses of mitochondriatargeted inhibitors blocked the enrichment of ALDH1<sup>bri+</sup> cells. These results suggested that resistant clones exhibiting CSC features relied upon mtOXPHOS for survival.

We then determined whether inhibition of mitochondrial respiration could counteract the intrinsic drug resistance mediated by CSC clones. At low doses, singleagent oligomycin A or tigecycline administration did

not induce substantial cell death, as measured by flow cytometry in PC9 T20 cells; however, when combined with gefitinib, the overall number of dead cells significantly increased. Indeed, in the presence of gefitinib, the lower dose of mitochondriatargeted inhibitors was equally effective as the higher dose (Figure 2G and Supplementary Figure S4H). These findings suggested that resistant CSCs were susceptible to the inhibition of the mitochondrial respiratory chain, and that oxidative metabolism could represent a prime target for overcoming TKI resistance in LAD.

#### The role of SIRT1 in the mitochondrial metabolism phenotype of TKI-resistant CSCs in LAD

To identify potential factors that regulate mtOXPHOS-mediated metabolic changes that occur in response to TKI exposure, we evaluated the effects of lentiviral vectormediated shRNA knockdown of SIRT1 in PC9 and HCC827 T20 cells, which was confirmed by immunoblot after use of two independent shRNAs for each gene (Supplementary Figures S5A and B). Knockdown of SIRT1 reduced mitochondrial respiratory capacities in PC9 and HCC827 T20 cells (Figure 3A). Additionally, mtDNA content was reduced upon SIRT1 ablation in PC9 and HCC827 T20 cells (Figure 3B). Moreover, transfection of SIRT1

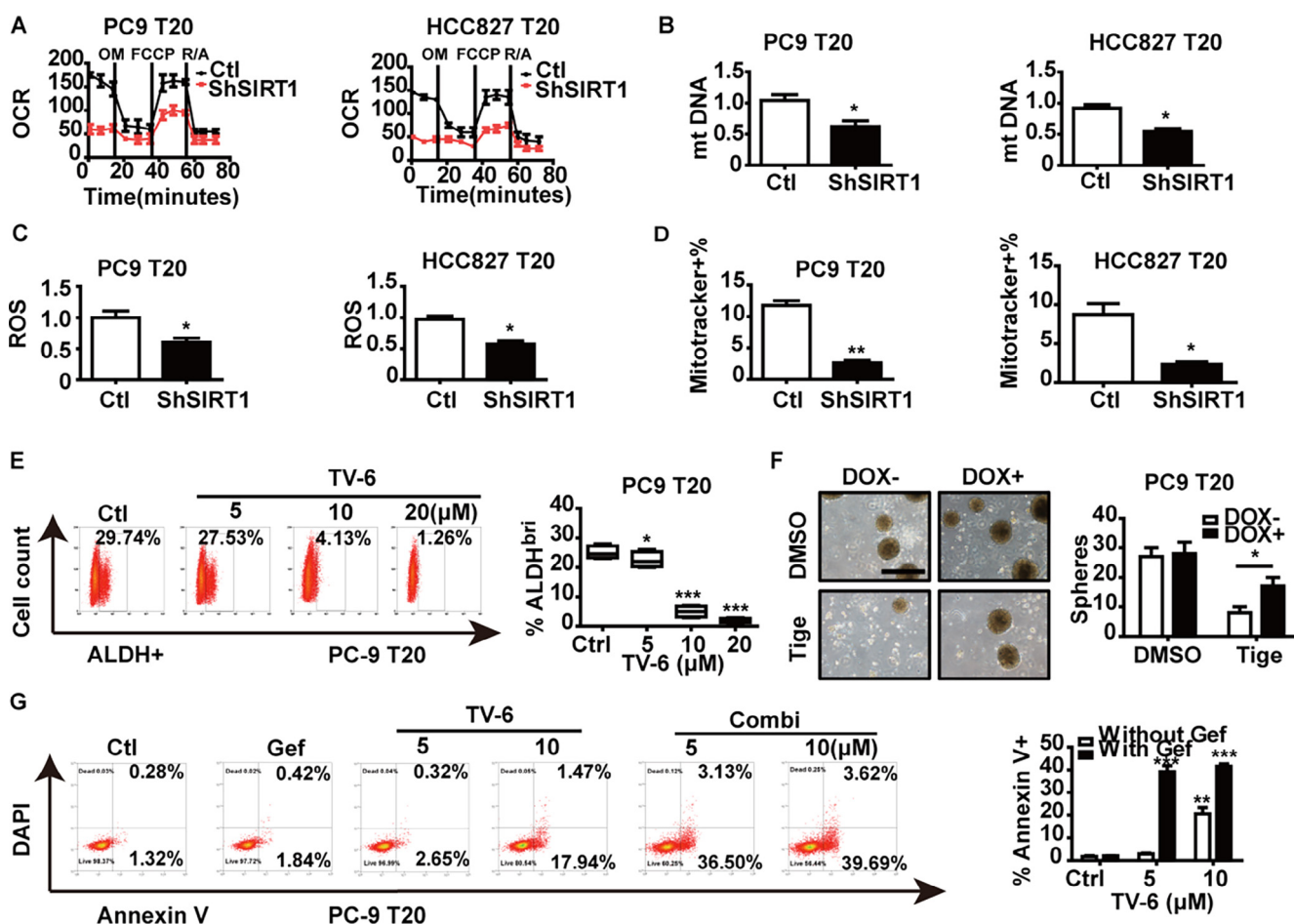


**Figure 3.** Inhibition of SIRT1 inhibits the mtOXPHOS dependency of CSCs. A, OCRs were determined by a Seahorse XFe96 extracellular flux analyzer. B, mtDNA levels were measured by real-time quantitative PCR. C, ROS levels were determined by ROS-Glo. D, LAD cell lines were stained with MitoTracker Red CMX Ros and then analyzed by flow cytometry. E, Relative percentage of the ALDH<sup>bri+</sup> subpopulation in PC9 T20 cells under TV-6 treatment at the indicated concentrations. F, PC9 T20 cells were seeded for sphere assays (40×) and were treated with DMSO or tigecycline DOX. The inhibitory effect of tigecycline on sphere formation was abolished in PC9 T20 cells expressing DOX-inducible SIRT1 as compared with uninduced cells. Scale bar = 500 μm. G, Flow cytometric determination of the frequency of the Annexin V<sup>+</sup> cell fraction in PC9 T20 cells treated with gefitinib (Gef) and/or TV-6 at the indicated concentrations. Annexin V was used as a marker of cell death. A representative result from three independent flow cytometry experiments is shown.

shRNA into PC9 and HCC827 T20 cells reduced ROS (Figure 3C) and mtMPs (Figure 3D) levels, and reductions in sphere formation (Supplementary Figure S5C) and the ALDH1<sup>bri+</sup> fraction (Supplementary Figure S5D) were also observed in PC9 and HCC827 T20 cells following SIRT1 ablation.

We then determined whether SIRT inhibitors could produce similar antitumor effects as observed with genetic strategies. To this end, we used the SIRT1 inhibitors TV6 and EX 527. Similar to SIRT1 ablation, TV6 reduced sphere formation (Supplementary Figure S5E) and the ALDH1<sup>bri+</sup> fraction (Figure 3E and Supplementary Figure S5F) of PC9 and HCC827 T20 cells and was associated with decreased oxygen consumption rate (OCR) (Supplementary Figure S5G), and mtMP (Supplementary Figure S5H). Similarly, EX 527 decreased sphere formation (Supplementary Figure S5I) and the ALDH1<sup>bri+</sup> fraction (Supplementary Figure S5J) of PC9 and HCC827 T20 cells and inhibited mitochondrial respiratory capacity as assessed by OCR (Supplementary Figure S6A) and mtMP (Supplementary Figure S6B).

Additionally, we found that the inhibitory effect of tigecycline on sphere formation was rescued in PC9 T20 cells expressing doxycycline (DOX)inducible *SIRT1* as compared with uninduced control cells (Figure 3F). Furthermore, the inhibitory effect of oligomycin A on stemness maintenance was also abolished in PC9 T20 cells stably overexpressing *SIRT1* as compared with control cells, suggesting that the tumorinitiating capacity potentiated by SIRT1 relies on mtOXPHOS (Supplementary Figure S6C). These results implied that SIRT1 potentiated mtOXPHOS and subsequent CSC enrichment.

Consequently, we then determined whether eliminating *SIRT1* expression could affect the responsiveness of LAD cells to anticancer drugs. Indeed, highdose TV6 modestly increased apoptosis in PC9 T20 cells resistant to TKI treatment, with this accompanied by a significant sensitization to gefitinib therapy. At a lowerdose, singleagent TV6 did not induce substantial cell death in PC9 T20 cells; however, the sensitization to anticancer approaches with lowdose TV6 in resistant cells was comparable to that achieved by highdose treatment (Figure 3G). Additionally, we confirmed SIRT1 inhibition as a combinatorial strategy to sensitize gefitinibinduced cell death using EX 527 (Supplementary Figure S6D).

Collectively, these findings indicated that SIRT1 inhibition enhanced the targeting of resistant CSCs in combination with molecular targeted drugs in LAD.

#### *TV-6 selectively targets CSCs and acts together with gefitinib to block tumor growth and prolong remission*

We tested the *in vivo* effect of TV6, gefitinib, and the combination of both on primary human PDXs initiated from a sample from a TKIrefractory LAD patient and engrafted in NSG mice. We first evaluated the pharmacokinetics of TV6 in mice (Supplementary Figure S7A), subsequently choosing a treatment schedule of twicedaily i.p. injections. Following engraftment, mice ( $n = 10$  mice/group) were treated after 14 days with a 3week course of gefitinib (100 mg/kg/day), TV6 (50 mg/kg/day), both drugs combined and vehicle only (Supplementary Figure S7B). We observed a synergistic response from combined TV6 and gefitinib treatment of tumors arising after 14 days. After 15 days of treatment, the drug combination virtually eliminated tumors, whereas injection of gefitinib alone had little effect on tumor remission. Moreover, mice treated with TV6 alone showed reduced tumor growth relative to that observed in untreated or gefitinibtreated mice, and after day 20, we observed only modest tumor regression. Furthermore, combined treatment resulted in further reductions in TV after an additional 20 days. In mice treated with TV6 alone, tumor growth was suppressed until day 40, after which tumor growth resumed and/or showed signs of relapse at rates near those observed in untreated control mice, whereas the major-

ity of mice receiving combined treatment with TV6 and gefitinib sustained low engraftment following drug withdrawal along with no detectable tumor for at least 65 days (Figure 4A and B). In all experimental arms, we observed no changes in the appearance or behavior of the mice or signs of myelosuppression (Figure 4C), thereby confirming excellent tolerability. Additionally, we found no alterations in serum levels of liver, muscle, or cardiac enzymes (Figure 4D).

Importantly, the ALDH1<sup>bri+</sup> fraction in residual PDXs decreased, although marginally, in gefitinibtreated mice but significantly in mice treated with TV6, with further reductions observed in mice receiving combined treatment with both drugs (Figure 4E), indicating that TV6 was active against CSCs. Secondary transplantation of residual tumor from mice receiving combined treatment resulted in significantly reduced engraftment relative to single agents, indicating a reduced CSC capacity of residual cells. Additionally, TV6 resulted in abrogation of secondary engraftment, whereas gefitinib treatment alone did not significantly affect engraftment in secondary recipients or CSC frequency (Supplementary Table S3). Furthermore, mice treated with TV6 demonstrated significantly improved survival after discontinuation of therapy as compared with control or gefitinibtreated mice, and combined therapy further increased survival as compared with single agent alone (Figure 4F).

We also evaluated the efficacy of TV6 or tigecycline in combination with gefitinib using the CalcuSyn median effect model, where the combination index (CI) indicates synergism ( $CI < 0.9$ ), additivity ( $CI = 0.9-1.1$ ), or antagonism ( $CI > 1.1$ ). Combined treatment with TV6 and gefitinib showed an additive or synergistic effect; however, when TV6 was added either before or after gefitinib, the combinatorial effect was clearly synergistic (Figure 4G). Similarly, treatment effects with tigecycline in combination with gefitinib were additive or synergistic, regardless of drug sequence (Figure 4H). Our findings suggest important implications for tumor treatment and pave the way for targeting OXPHOS or SIRT1 in association with oncogenic pathway inhibitors to eradicate CSCs and prevent tumor relapse in LAD.

#### *TV-6 reduces the gefitinib dose necessary to prolong remission and decrease lung colonization*

Because cytotoxic therapy is toxic and causes unwanted and often serious side effects in cancer patients [23], a major challenge is to lower the doses of TKIs without decreasing their effectiveness. We reasoned that the combinatorial effect of TV6 might permit lowering of the gefitinib dose. To test this hypothesis, we transplanted nude mice subcutaneously with PC9 cells carrying a luciferase reporter and evaluated the effects of a 3week course of scheduled treatments starting 14 days later when tumors were already palpable ( $n = 10$  mice/group). We administered gefitinib (100 mg/kg/day), TV6 (50 mg/kg/day), both drugs combined, as well as TV6based combinatorial therapy involving a fourfold reduced concentration of gefitinib (25 mg/kg/day instead of 100 mg/kg/day) (Supplementary Figure S8A). As monotherapies, treatment of PC9 xenografts with higherdose gefitinib suppressed tumor growth but did not prevent relapse. However, the reduced dose of gefitinib alone was less effective, as tumor regression was not observed. Interestingly, combined treatment with TV6 and the reduced dose of gefitinib resulted in complete tumor regression and no detectable relapse for at least 65 days. Indeed, in the presence of TV6, the lower dose of gefitinib was equally as effective as the higher dose in prolonging remission (Figure 5A-C).

We then determined the effect of different dosing schedules on the lung engraftment of PC9 cells intravenously injected into the tail of nude mice (Supplementary Figure S8B). For imaging of lung metastatic activity and distribution, mice were viewed dorsally and ventrally by bioluminescence imaging weekly, as well as by examination of the lungs at necropsy.

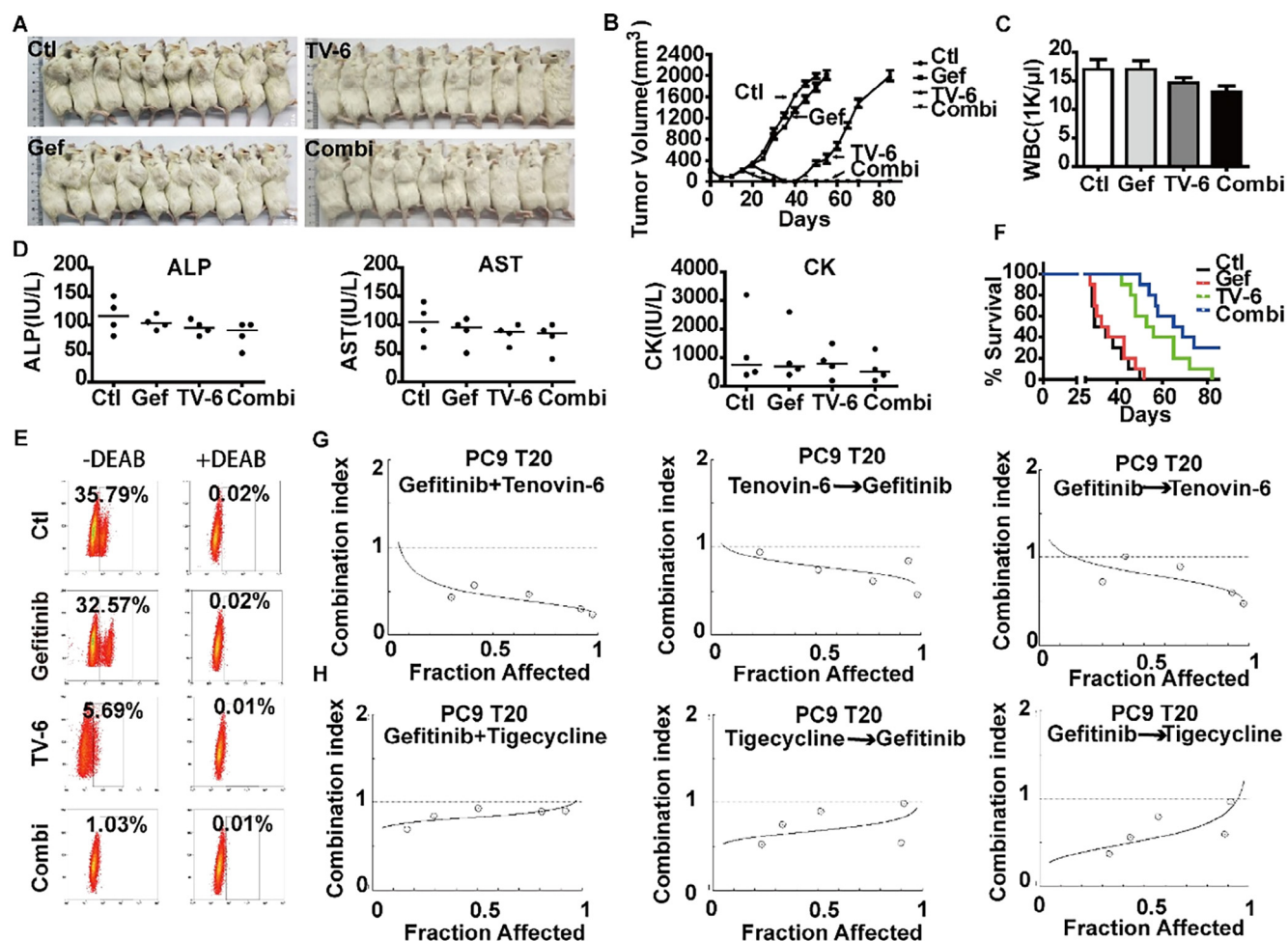


**Figure 4.** SIRT1 inhibitor(s) target CSCs and act synergistically with gefitinib to reduce tumor growth in vivo. A and B, Representative images of subcutaneous PDXs in mice at day 40 for each group. Plots of tumor-growth curves. There was a significant size reduction in tumors treated with TV-6 or both TV-6 and gefitinib as compared with that in control or gefitinib-only groups. C, The total white blood cell count in mice after discontinuation of treatment. D, Serum levels of liver enzymes [alkaline phosphatase (ALP), aspartate aminotransferase (AST), and creatine kinase (CK)] in mice from each group. Lines represent medians. E, Cells were dissociated from tumors and subjected to Aldefluor assay. The percentage of ALDH<sup>br</sup> cells is shown. F, Survival of mice from (A) after discontinuation of treatment. G and H, The viability of PC9 T20 cells after different treatments with gefitinib (Gef) combined with TV-6 (G) or tigecycline (H) according to MTS assay. Data were analyzed with CalcuSyn software to generate a CI versus fractional effect (cell death) plot showing the effect of the combination of Gef with TV-6 or tigecycline. CI < 1 indicates synergism.

A single dose of TV6 was more effective at inhibiting tumor colonization than gefitinib alone at a dose of 25 mg/kg. Moreover, 100 mg/kg gefitinib as a single agent potentially lowered lung bioluminescence signals, whereas lowdose gefitinib mice were moribund and presented enlarged lung engraftment of GFP<sup>+</sup> cells, which did not occur in mice receiving highdose therapy. Indeed, decreased engraftment upon treatment was sharply accelerated by combined treatment with TV6 and gefitinib, with a slightly more pronounced effect observed with the higher gefitinib dose than the lower dose. However, the absence of relapse due to TV6 therapy was comparable at both doses of gefitinib for the period of the experiment. A double dose of gefitinib plus TV6 substantially reduced longterm lung engraftment, and the number of colonies remained at almost undetectable levels, even after up to 53 days (Figure 5D and E; Supplementary Figure S8C). These preclinical observations suggested the possibility of using SIRT1 inhibitors to lower the gefitinib dose in LAD patients.

Similar to the results obtained from bioluminescence lungcolonization experiments, mice treated with highdose gefitinib monotherapy or combined TV6 and gefitinib showed a dramatic decrease in the number of nodules and incidence of lung metastasis as compared with mice treated

with other schedules (Figure 5F). Furthermore, decreased frequency of metastasis was confirmed by a significant reduction in histologically determined organ infiltration of tumor cells into the lungs of these mice relative to that observed in those bearing more nodules. The infiltration of tumor cells between different dosages was more pronounced at 21 days after drug withdrawal when lowdose gefitinibtreated mice were moribund and displayed massive lung infiltration of tumor cells, which did not occur in those receiving highdose therapy and/or combined treatment (Figure 5G).

These results indicated that adding mitochondrial inhibitors to firstline TKI treatment significantly diminished the number of cells with high repopulation and invasion potential, and that even relatively lowdose TKI treatment could yield a sustained antitumor effect.

#### *Inhibition of metabolic activity prevents the development of drug resistance*

Given the hypersensitivity of TKI-resistant cells to metabolic inhibitors and the metabolic reprogramming present in resistant cells, we determined whether metabolic inhibitors and TKI therapy could synergistically pre-

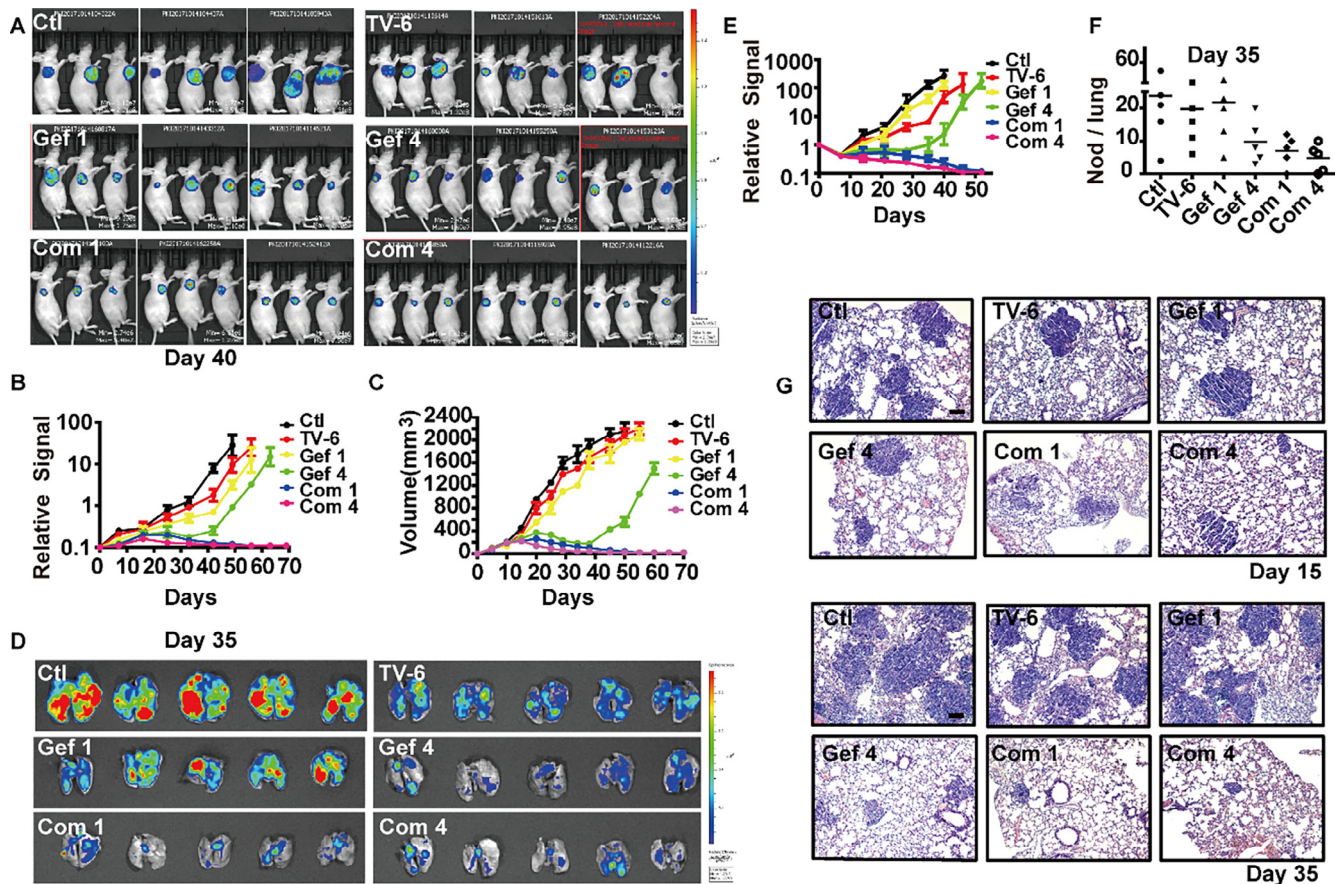


**Figure 5.** TV-6 reduces the gefitinib dose necessary to prolong remission and decrease lung colonization. A and B, Normalized bioluminescence signals of tumor remission and representative bioluminescence images of mice injected subcutaneously with PC9 cells carrying a luciferase reporter and treated with different dosage schedules at day 40 post-administration. The data represent the average SEM. C, Tumor-growth curves of tumor-bearing nude mice following receipt of the indicated dosage schedules. D and E, Normalized bioluminescence signals of lung metastatic nodules and representative bioluminescence images of lungs injected with PC9 cells carrying a luciferase reporter and treated with different dosage schedules at day 35 post-administration. Data represent the average SEM. F, Column scatter plot showing the number of surface metastases per lung in mice receiving the indicated dosage schedules. G, Tumor infiltration into lung tissue in nude mice treated with different schedules was analyzed at 15 and 35 days post-administration of drug(s) according to H&E-stained lung sections. Scale bar = 100  $\mu$ m.

vent the emergence of acquired drug resistance. We examined the ability of a subset of putative anticancer compounds to prevent the emergence of tolerant colonies by cotreating cultures continuously with gefitinib and these compounds. Among the tested compounds, three different SIRT1 inhibitors as well as mitochondrial metabolism inhibitors virtually eliminated the emergence of drug-tolerant colonies from PC9 cells during anti-tumor treatment, whereas other tested agents did not in the presence of gefitinib (Figure 6A and B). This result presented a new therapeutic opportunity for not only targeting resistant LADs but also to possibly prevent the emergence of resistant subpopulations and achieve greater response from sensitive LADs treated with first-line TKIs. Upon pretreatment of nave PC9 cells with tigecycline for 5 days, followed by immediate removal of the inhibitor before isolating individual cells by transfer to sixwell plates, we were unable to detect any TKI-tolerant clones (Figure 6C). However, pretreatment of nave cells and removal of the inhibitor 72 h prior to isolating individual cells allowed detection of TKI-tolerant clones in a proportion similar to that observed in control nave cells (Figure 6D), suggesting that drug-tolerant cells were continuously replenishing in the absence of agents eliminating them. This suggested that preexisting TKI-tolerant cells in nave LAD populations are highly metabolism dependent.

#### *Clinical significance of the expression of SIRT1 and mtOXPHOS components in LAD patients*

We used an independent series of tumors derived from LAD patients sensitive to first-generation TKIs or exhibiting relapse characteristics under gefitinib treatment to determine levels of SIRT1, ALDH1, and widely accepted stem cell markers of lung cancer and a subset of mtOXPHOS components by immunohistochemistry (IHC) (Figure 7A). These mtOXPHOS proteins include, cytochrome C oxidase IV, a component of mitochondrial complex IV and a frequently used marker for mitochondrial content, PGC1 $\alpha$ , a transcriptional coactivator that promotes energy metabolism and ROS detoxification, and mitochondrial ribosomal protein S5, which localizes to the mitochondria and promotes complex I function and NAD<sup>+</sup> generation to enhance mitochondrial respiration. Our results identified markedly higher levels of SIRT1, ALDH1, and mtOXPHOS components in sections from postrelapse tumor tissues as compared with TKI-naïve samples.

We then analyzed the clinical relevance of SIRT1 and CSC marker expression in human LAD samples. Based on the expression levels, samples were divided into two groups (SIRT1/ALDH1<sup>high</sup> and SIRT1/ALDH1<sup>low</sup>). SIRT1 and ALDH1 expression was significantly associated

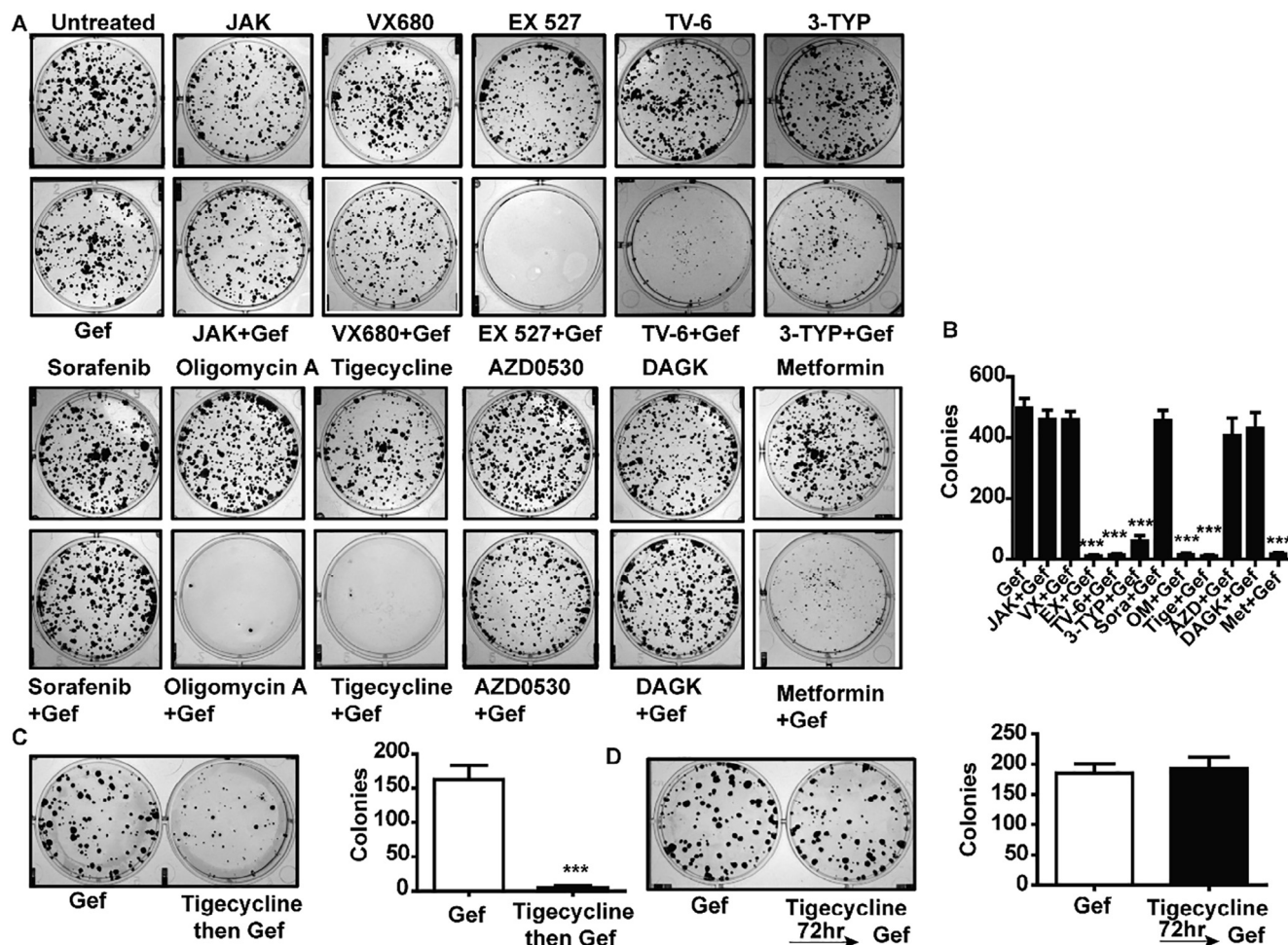


**Figure 6.** Preventing the Establishment of Drug-Tolerant Clones. A, PC9 cells were either untreated or treated alone with the indicated pharmacological agents for 7 days (top rows) or with Gefitinib (Gef) alone or the combination of the indicated agent with Gefitinib for 40 days (bottom rows). Fresh media with drugs were provided every 3 days. Following treatment, plates were fixed and stained. All experiments were performed in triplicate and representative plates are shown. B, Individual colonies were counted and the quantified results were graphed. In some cases the colonies were too numerous to count (indicated as > 500 colonies). Error bars represent standard deviations from the mean of three independent experiments. C, PC9 cells were either treated with Gefitinib (Gef) for 30 days or pretreated for 5 days with Tigecycline and then immediately treated with Gefitinib for 30 days, plates were fixed and stained. D, PC9 cells were either treated with Gefitinib for 30 days, in addition, pretreated for 5 days with Tigecycline, then removed the inhibitor 72 hours prior to Gefitinib treatment for 30 days. Plates were fixed and stained. The experiment was performed in triplicate and representative plates are shown.

with multiple aggressive clinicopathological characteristics, such as large tumor size, high recurrence and metastasis rates, and cancer embolus (Figure 7B). Moreover, Kaplan–Meier survival analysis indicated that compared with the SIRT1/ALDH1<sup>low</sup> profile, LAD patients with the SIRT1/ALDH1<sup>high</sup> profile had a much worse prognosis (Figure 7C).

These data suggested that the SIRT1/mtOXPHOS protein axis plays a critical role in predicting resistance to TKI and poor prognosis in LAD patients.

## Discussion

Targeting oncogened driven signaling pathways represents a clinically validated approach to treating several devastating diseases; however, despite such treatments resulting in significant tumor shrinkage, the frequency of relapse remains. Insights into the limitations of targeted kinase therapy were obtained from understanding that LAD comprises differentiated cells, as well as a higher fraction of spherogenic and tumorigenic undifferentiated cells that survive shutdown of oncogenic signaling and

are capable of propagating the disease [1,3]. Using multiple treatment cycles, we developed a series of progressively resistant cell lines representing different oncogenotypes, followed by molecular characterization of the entire series and identification of novel pathways involving an increased dependency on mitochondrial biogenesis and oxidative phosphorylation. Previous studies also revealed a metabolic vulnerability to tumor recurrence following neoadjuvant chemotherapy via molecular profiling of residual disease [24,25].

Tumor cells reprogram a variety of central metabolic and bioenergetic pathways to maintain exacerbated growth and survival rates [6]. Several recent reports explored mitochondrial respiration specificities as targetable susceptibilities of cytotoxic drugselected CSCs, which when exploited, should be synthetically lethal when combined with established therapies [8]. For example, residual breast cancers after conventional chemotherapy display mtOXPHOS, as well as tumorinitiating features [26]. Mammospheres obtained from hormonedependent, estrogenreceptorpositive breast cancer exhibit upregulation of key mitochondrial enzymes involved in oxidation and ketone metabolism [27], suggesting that CSC metabolism

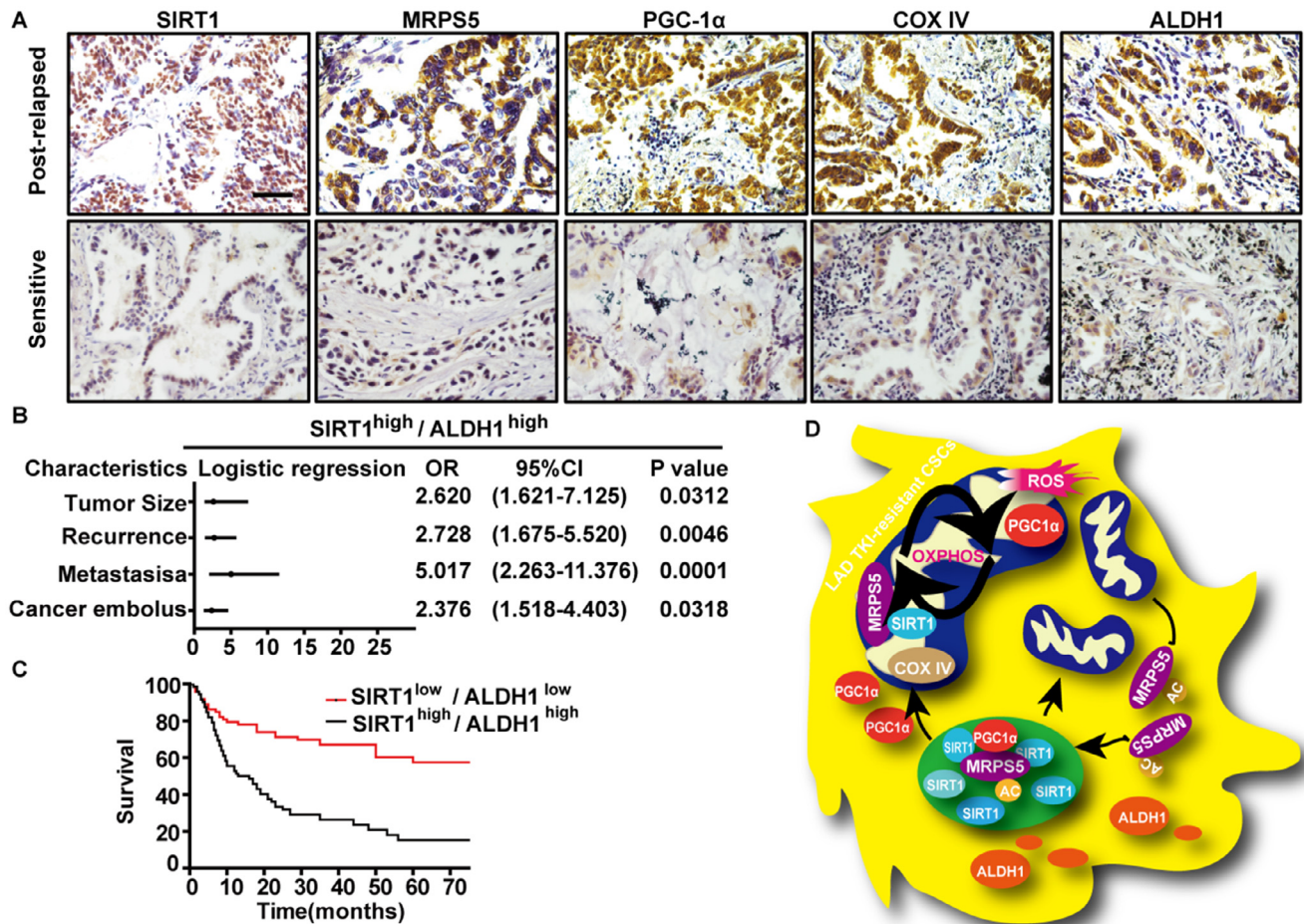


**Figure 7.** Clinical significance of the expression of SIRT1 and mtOXPHOS components in LAD patients. **A**, Representative results of IHC staining for SIRT1, mtOXPHOS components, and ALDH1. Case 1 (upper panel): sample from a post-relapsed LAD patient under gefitinib treatment; and case 2 (lower panel): TKI-naïve LAD sample harboring an EGFR mutation. Scale bar, 25  $\mu$ m. **B**, Based on IHC staining results, clinical samples were divided into two groups: SIRT1<sup>high</sup>/ALDH1<sup>high</sup> and SIRT1<sup>low</sup>/ALDH1<sup>low</sup>. Multivariate logistic regression analysis of the odds ratios for different clinicopathological characteristics showed that compared with the low profile, patients with the high profile had a higher risk of large tumor size, recurrence, metastases, and cancer embolus. **C**, Kaplan–Meier analysis of the association between SIRT1/ALDH1 levels and the overall survival rate of LAD patients. **D**, A theoretic model underlying the role of the SIRT1-mtOXPHOS axis in LAD metabolic reprogramming and stemness maintenance. Evaluation of LAD cell populations treated with the TKI inhibitor gefitinib identified unique aspects of a subpopulation of tumor cells exhibiting stem-like properties and mitochondria-specific metabolic features along with their reliance on sirtuin 1 (SIRT1) for survival advantage. Inhibition of SIRT1 and mitochondrial oxidative phosphorylation (mtOXPHOS) blocks CSC expansion and restores TKI sensitivity.

relies on mitochondrial respiration. Vazquez et al. [28] report reduced glycolysis and increased OXPHOS in certain melanomas, revealing metabolic plasticity rather than stable Warburg pathophysiology. Furthermore, Haq [11] reported that increased OXPHOS is required for melanomas to survive BRAF inhibition, suggesting the potential benefit of investigating therapeutic combinations of BRAF inhibitors with metabolism-related inhibitors. Other studies [9,29,30] showed that leukemic primitive cells rely more heavily on OXPHOS to supply their energetic demands as compared with bulk tumor cells, thereby suggesting a link between mitochondrial pathophysiology and therapy resistant clones and representing an attractive topic for future investigation. Furthermore, using singlecell RNA sequencing coupled with a highly sensitive BCR–ABL detection method, Giustacchini et al. [31] showed that primitive BCR–ABL<sup>+</sup> cells from chronic myelogenous leukemia (CML) patients presented an overexpression of OXPHOS and fatty acid oxidation-related genes as compared with BCRABL counterparts. This suggests that the oxidative phenotype characterized in the present study is specific to leukemia stem cells in

patients, further highlighting the clinical relevance of our findings. Our findings identified an adaptive metabolic program that limits the therapeutic efficacy of EGFR inhibitors. Intrinsic resistance conferred by metabolic specificities could represent an additional protective mechanism that helps cells survive the initial contact with various cytotoxic agents and provides cells with added survival time to establish longer-lasting secondary resistance mechanisms (Figure 7D).

A previous study demonstrated that SIRT1 deacetylates the mitochondrial master regulator PGC1 $\alpha$  to enhance mtDNA replication and biogenesis [32]. Interestingly, PGC1 $\alpha$  inhibition did not directly inhibit CML hematopoiesis, suggesting that additional SIRT1-related mechanisms besides regulation of mitochondrial respiration are also involved in promoting CML stem cell growth. Although the role of SIRT1s in oncogenesis varies based on tissue type, recent evidence revealed a critical function for SIRT1 in regulating p53 deacetylation in CML-specific escape from imatinib therapy [20]. To gain further insights into SIRT1, they extended their findings and proposed a mechanism involving a positive feedback

loop between SIRT1 and cMYC in regulating acute myeloid leukemia (AML) stem cells harboring a FLT3 internal tandem duplication mutation [19]. In the future, it will be of interest to explore interactions between SIRT1 regulation of metabolism and its regulation of p53 and cMYC and those effects on CSCs in LAD. Although changes in chromatin in our study were reminiscent of an established model of drug-tolerant lung cancer cells, the underlying mechanisms appeared distinct, as we did not observe enrichment of KDM5A in LAD cells that survived acute, short-term exposure to an EGFR inhibitor [33]. It is possible that additional chromatin-modifying enzymes contribute to TKI tolerance in various experimental contexts. A plausible explanation is the involvement of unknown oncogenic signaling pathways activated by *EGFR* mutants that arise from the adaptation of cells from prolonged exposure to TKIs. The discrepancy further highlights the importance of understanding under which cellular context and protein complexes these enzymes act and suggests that differences in genetic backgrounds, culture conditions, specific oncogenes present, and the use of knockdown constructs versus the study of knockout cells must be taken into account.

Interestingly, it was recently reported that a subpopulation of pancreatic cancer cells that had survived *Kras* ablation were also mainly dependent on OXPHOS [12]. Similarly, treatment of *BRAF*-mutated melanomas with *BRAF* inhibitors renders them addicted to OXPHOS [10,11]. This observation together with the results of the present study indicate that in oncogene-expressing tumors, there exists a small subpopulation endowed with tumorigenic potential, self-renewal capabilities, intrinsic resistance to targeted therapies, high hyperpolarized mitochondria, and increased consumption of oxygen. By contrast, another study found that human CSCs derived from a large panel of PDX models carrying activating *KRAS* mutations identical to those found in their bulk counterparts bear distinct metabolic phenotypes with limited plasticity and controlled by *MYC* [34]. Strikingly, CSCs from a second PDX model carrying wildtype *KRAS* showed a similar metabolic phenotype, further corroborating that the lack of plasticity is independent of *KRAS* mutational status. Moreover, *KRAS*-ablated cells require reactivation of mutant *KRAS* for proliferation and tumor relapse, suggesting that the observed OXPHOS phenotype is restricted to oncogene-ablated dormant cells (as described in the present study), as opposed to the highly tumorigenic CSCs studied by others. The metabolic phenotype of CSCs appears not to be universal but rather varies according to context. Elucidating the molecular basis for this specificity with regard to differential oncogenic reprogramming of cellular metabolism will be the next critical step in understanding tumor heterogeneity and complexity.

The CSC hypothesis is based on the differential tumor-forming properties and responses to well-defined therapy [35]. A prediction of this model, heretofore untested, is that drugs that selectively inhibit CSCs should function synergistically with well-defined drugs to prolong the therapeutic response and make them more susceptible to a second drug. Additionally, it might have a potential use in preventing the development of drug tolerance, as opposed to treating resistance that has already occurred. Based on our findings, the addiction to OXPHOS treated with EGFR-targeted therapy suggests that mitochondrial inhibitors should be evaluated in combination with EGFR-pathway inhibitors *in vivo*. Upon drug withdrawal, we observed regression of transplanted tumors following single-agent treatment within 2 to 3 weeks, followed by relapse after 5 to 6 weeks; however, combinatorial therapy involving TV6 prevented relapse for at least 2 months and indeed might have even represented a cure for these xenograft-generated tumors. Another major problem that cancer patients face is the high toxicity of conventional and molecularly-targeted drugs that manifest as anemia, appetite changes, fatigue, hair loss, nausea, vomiting, and fertility changes [23]. By contrast, lower doses of these well-defined therapeutics are ineffective at suppressing tumor burden. Therefore, identification of agents that can be combined with lower doses of existing ther-

apeutics is of high clinical relevance. Although TV6 is not a candidate for drug development targeting tumor regression, our observations support further investigation of SIRT1 inhibition as an approach for targeting LAD CSCs in combination with TKI treatment. TV6 exhibited comparable effects in preventing relapse and prolonging the therapeutic response when combined with a fourfold reduced dose of gefitinib, which was ineffective as a monotherapy. Therefore, TV6 exhibited broad anticancer effects of potential utility in a wide variety of clinical contexts for both cancer treatment and lowering the toxicity associated with first-line TKI therapy. Recent studies focusing on tolerance to SIRT1 inhibitors showed that TV6 appeared more tolerable to normal hematopoietic progenitor cells according to multiple endpoints, and that applying it as a treatment in combination with the BCRABL TKI imatinib promoted eradication of CML stem cells in mouse models [19,20]. Within the limited scope of the present study, we observed no changes in body or spleen weight or signs of toxicity during treatment, and total bone marrow cellularity was unaffected in all experimental arms, thereby confirming excellent tolerability. These observations, although preliminary, indicate promising avenues for further investigation toward using a combination of TV6 and gefitinib to eliminate residual CSCs, as well as determine the safety and tolerability in patients with LAD who are in cytogenetic remission with evidence of residual EGFR<sup>+</sup> cells. Furthermore, our model identified clinically relevant mechanisms of drug resistance; therefore, the mouse model could be a surrogate for acquired TKI drug resistance, as it captures cells that persist following a single cycle of TKI therapy and could, therefore, mimic a patient that clears the vast majority of the bulk population but experiences regrowth of disease within months of starting therapy. Additionally, the model could offer insight into mechanisms of relapse. The high OXPHOS status not only correlated with the probability of achieving remission with induction TKI therapy in an independent dataset of patients with LAD but also correlated with overall survival, thereby supporting the clinical relevance of our findings. Moreover, this model is compatible with recent findings by Farge et al. [29], which demonstrated an *in vivo* approach to identifying primary AML cells that persist in the bone marrow after chemotherapy. In that study, mice were engrafted with tumor cells and then treated with cytarabine at an appropriate dose and schedule to reduce the level of tumor burden. On the time interval of maximal depletion of tumor cells, the residual disease that persisted in the mouse bone marrow was isolated and studied.

Some potential limitations should be considered in our findings. First, the *in vitro* and *in vivo* studies of CSC response to TKIs and SIRT1 inhibitors were confined to a relatively small number of patient samples. Consequently, these data are not robust, and the results must, therefore, be interpreted with due caution. Additionally, LAD CSC populations vary from patient to patient, which can directly affect the response or resistance of these cells to single and combined treatments. Another consideration is the off-target effects of the SIRT1 inhibitor. All SIRT inhibitors, including TV6, suppress more than SIRT1 [36]; therefore, results from use of SIRT inhibitors should be interpreted with multiple enzymes in mind. This raises the question as to whether functional redundancy exists within SIRT families based on sequence homologies and architectural similarities. Although difficult to reconcile, discrepancies might at least be due to the fact that no study has demonstrated selective inhibition of the SIRT1 deacetylase, despite recent studies of several mechanism-based inhibitors targeting SIRT histone deacetylases. Although we cannot exclude the possibility that TV6 also suppresses other SIRTs, these results could also be faithfully reproduced using an independent SIRT1 shRNA approach and tumor cells to distinguish the phenocopying effects of the chemical inhibitor. This could support SIRT1 as at least one target mediating TV6 effects. Even with these considerations, the clinical implication of this work provides a supportive rationale for blocking the mtOXPHOS pathway in *EGFR*-mutant LAD patients and specifically in those who

developed resistance under antiEGFR therapy. Further work will reveal whether there are practical opportunities for synthetic lethality by pharmacology limiting the adaptive ability of transformed cells to upregulate OXPPOS when facing stress, such as oncogenic kinase inhibition.

## Authors contributions

Conception and design: Xiang Yuan, Jiangtao Sun;

Development of methodology: Yiwen Liu, Jinyu Kong, Guifang Li, Mingyang Ma, Kaifang Song;

Acquisition of data (acquired and managed patients, provided facilities, etc.): Jiangtao Sun, Guifang Li, Kaifang Song;

Analysis and interpretation of data (e.g., statistical analysis, biostatistics, computational analysis): Jinyu Kong, Yiwen Liu, Guifang Li, Huaxu Li, Kaifang Song;

Writing, review, and/or revision of the manuscript: Jiangtao Sun, Xiang Yuan, Daxing Zhu, XiaoJun Tang;

Administrative, technical, or material support (i.e., reporting or organizing data, constructing databases): Xiang Yuan, Guifang Li, Yiwen Liu, Jinyu Kong, Mingyang Ma;

Study supervision: Xiang Yuan.

## Funding

This work was supported in part by grants from the National Natural Science Foundation of China (U1404817 and 81702820 for Xiang Yuan), Young academic leaders of Henan University of Science and Technology (for Xiang Yuan), China Postdoctoral Science Foundation (171234 for Xiang Yuan), Project of Henan Provincial Department of Health (201504037 for Jiangtao Sun).

## Acknowledgments

The authors gratefully thank Dr. Chen at the University of Pittsburgh (Pittsburgh, PA) and Dr. Cao at the University of California Los Angeles (Los Angeles, CA), for their help in experimental technologies and for critically editing a draft of this article.

## Appendix A. Supplementary data

Supplementary data to this article can be found online at <https://doi.org/10.1016/j.neo.2019.10.006>.

## References

1. Tan CS, Gilligan D, Pacey S. Treatment approaches for EGFR-inhibitor-resistant patients with non-small-cell lung cancer. *Lancet Oncol* 2015;**16**: e447–59.
2. Remon J, Besse B. Unravelling signal escape through maintained EGFR activation in advanced non-small cell lung cancer (NSCLC): new treatment options. *ESMO Open* 2016;**1**: e000081.
3. Zhou BB, Zhang H, Damelin M, Geles KG, Grindley JC, Dirks PB. Tumour-initiating cells: challenges and opportunities for anticancer drug discovery. *Nat Rev Drug Discov* 2009;**8**:806–23.
4. Huang CP, Tsai MF, Chang TH, Tang WC, Chen SY, Lai HH, Lin TY, Yang PC, Yang PC, Shih JY, et al. ALDH-positive lung cancer stem cells confer resistance to epidermal growth factor receptor tyrosine kinase inhibitors. *Cancer Lett* 2013;**328**:144–51.
5. Morgillo F, Della Corte CM, Fasano M, Ciardiello F. Mechanisms of resistance to EGFR-targeted drugs: lung cancer. *ESMO Open* 2016;**1**: e000060.
6. Tennant DA, Duran RV, Gottlieb E. Targeting metabolic transformation for cancer therapy. *Nat Rev Cancer* 2010;**10**:267–77.
7. Dorr JR, Yu Y, Milanovic M, Beuster G, Zasada C, Dabritz JH, Lisee J, Lenze A, Gerhardt A, Schleicher K, et al. Synthetic lethal metabolic targeting of cellular senescence in cancer therapy. *Nature* 2013;**501**:421–5.
8. Wolf DA. Is reliance on mitochondrial respiration a chink in the armor of therapy-resistant cancer? *Cancer Cell* 2014;**26**:788–95.
9. Kuntz EM, Baquero P, Michie AM, Dunn K, Tardito S, Holyoake TL, Helgason GV, Gottlieb E. Targeting mitochondrial oxidative phosphorylation eradicates therapy-resistant chronic myeloid leukemia stem cells. *Nat Med* 2017;**23**:1234–40.
10. Roesch A, Vultur A, Bogeski I, Wang H, Zimmermann KM, Speicher D, Korbel C, Laschke MW, Gimotty PA, Philipp SE, et al. Overcoming intrinsic multidrug resistance in melanoma by blocking the mitochondrial respiratory chain of slow-cycling JARID1B(high) cells. *Cancer Cell* 2013;**23**:811–25.
11. Haq R, Shoag J, Andreu-Perez P, Yokoyama S, Edelman H, Rowe GC, Frederick DT, Hurley AD, Nellore A, Kung AL, et al. Oncogenic BRAF regulates oxidative metabolism via PGC1alpha and MITF. *Cancer Cell* 2013;**23**:302–15.
12. Viale A, Pettazoni P, Lyssiotis CA, Ying H, Sanchez N, Marchesini M, Carugo A, Green T, Seth S, Giuliani V, et al. Oncogene ablation-resistant pancreatic cancer cells depend on mitochondrial function. *Nature* 2014;**514**:628–32.
13. Martin MJ, Eberlein C, Taylor M, Ashton S, Robinson D, Cross D. Inhibition of oxidative phosphorylation suppresses the development of osimertinib resistance in a preclinical model of EGFR-driven lung adenocarcinoma. *Oncotarget* 2016;**7**:86313–25.
14. Fernandez HR, Gadre SM, Tan M, Graham GT, Mosaoa R, Ongkeko MS, Kim KA, Riggins RB, Parasido E, Petrini I, et al. The mitochondrial citrate carrier, SLC25A1, drives stemness and therapy resistance in non-small cell lung cancer. *Cell Death Differ* 2018;**25**:1239–58.
15. Gerhart-Hines Z, Rodgers JT, Bare O, Lerin C, Kim SH, Mostoslavsky R, Alt Z, Wu Z, Puigserver P. Metabolic control of muscle mitochondrial function and fatty acid oxidation through SIRT1/PGC-1alpha. *EMBO J* 2007;**26**:1913–23.
16. Cant C, Gerhart-Hines Z, Feige JN, Lagouge M, Noriega L, Milne JC, Elliott P, Puigserver P, Auwerx J. AMPK regulates energy expenditure by modulating NAD+ metabolism and SIRT1 activity. *Nature* 2009;**458**(7241):1056–60. <https://doi.org/10.1038/nature07813>.
17. Kume S, Uzu T, Horiike K, Chin-Kanasaki M, Isshiki K, Araki S, Sugimoto T, Haneda M, Kashiwagi A, Koya D. Calorie restriction enhances cell adaptation to hypoxia through Sirt1-dependent mitochondrial autophagy in mouse aged kidney. *J Clin Invest* 2010;**120**:1043–55.
18. Ban J, Aryee DN, Fourtouna A, van der Ent W, Kauer M, Niedan S, Machado C, Rodriguez-Galindo C, Tirado OM, Schwentner R, et al. Suppression of deacetylase SIRT1 mediates tumor-suppressive NOTCH response and offers a novel treatment option in metastatic Ewing sarcoma. *Cancer Res* 2014;**74**:6578–88.
19. Li L, Osdal T, Ho Y, Chun S, McDonald T, Agarwal P, Lin A, Chu S, Qi J, Li L, et al. SIRT1 activation by a c-MYC oncogenic network promotes the maintenance and drug resistance of human FLT3-ITD acute myeloid leukemia stem cells. *Cell Stem Cell* 2014;**15**:431–46.
20. Li L, Wang L, Li L, Wang Z, Ho Y, McDonald T, Holyoake TL, Chen W, Bhatia R. Activation of p53 by SIRT1 inhibition enhances elimination of CML leukemia stem cells in combination with imatinib. *Cancer Cell* 2012;**21**:266–81.
21. Abraham A, Qiu S, Chacko BK, Li H, Paterson A, He J, Agarwal P, Shah M, Welner R, Darley-Usmar VM, et al. SIRT1 regulates metabolism and leukemogenic potential in CML stem cells. *J Clin Invest* 2019;**129**:2685–701.
22. Vandecasteele SJ, Seneca S, Smet J, Reynders M, De Ceulaer J, Vanlander AV, van Coster R. Tigecycline-induced inhibition of mitochondrial DNA translation may cause lethal mitochondrial dysfunction in humans. *Clin Microbiol Infect* 2018;**24**(4):431.e1–3. <https://doi.org/10.1016/j.cmi.2017.08.018>.
23. Drews RE, Shulman LN. Update in hematology and oncology. *Ann Intern Med* 2010;**152**:655–62.
24. Balko JM, Giltman JM, Wang K, Schwarz LJ, Young CD, Cook RS, Owens P, Sanders ME, Kuba MG, Sanchez V, et al. Molecular profiling of the residual disease of triple-negative breast cancers after neoadjuvant chemotherapy identifies actionable therapeutic targets. *Cancer Discov* 2014;**4**:232–45.

25. Boyd AL, Aslostovar L, Reid J, Ye W, Tanasijevic B, Porras DP, Shapovalova M, Almakadi M, Foley R, Leber B, et al. Identification of chemotherapy-induced leukemic-regenerating cells reveals a transient vulnerability of human AML recurrence. *Cancer Cell* 2018;**34**(483–498) e485.
26. Lee KM, Giltnane JM, Balko JM, Schwarz LJ, Guerrero-Zotano AL, Hutchinson KE, Nixon MJ, Estrada MV, Sanchez V, Sanders ME, et al. MYC and MCL1 cooperatively promote chemotherapy-resistant breast cancer stem cells via regulation of mitochondrial oxidative phosphorylation. *Cell Metab* 2017;**26**:633–47.
27. Lamb R, Harrison H, Hulit J, Smith DL, Lisanti MP, Sorgia F. Mitochondria as new therapeutic targets for eradicating cancer stem cells: Quantitative proteomics and functional validation via MCT1/2 inhibition. *Oncotarget* 2014;**5**:11029–37.
28. Vazquez F, Lim JH, Chim H, Bhalla K, Girnun G, Pierce K, Clish CB, Granter SR, Widlund HR, Spiegelman BM, et al. PGC1alpha expression defines a subset of human melanoma tumors with increased mitochondrial capacity and resistance to oxidative stress. *Cancer Cell* 2013;**23**:287–301.
29. Farge T, Saland E, de Toni F, Aroua N, Hosseini M, Perry R, Bosc C, Sugita L, Stuani L, Fraisse M, et al. Chemotherapy-resistant human acute myeloid leukemia cells are not enriched for leukemic stem cells but require oxidative metabolism. *Cancer Discov* 2017;**7**:716–35.
30. Skrtic M, Sriskanthadevan S, Jhas B, Gebbia M, Wang X, Wang Z, Hurren R, Jitkova Y, Gronda M, Maclean N, et al. Inhibition of mitochondrial translation as a therapeutic strategy for human acute myeloid leukemia. *Cancer Cell* 2011;**20**:674–88.
31. Giustacchini A, Thongjuea S, Barkas N, Woll PS, Povinelli BJ, Booth CAG, Sopp P, Norfo R, Rodriguez-Meira A, Ashley N, et al. Single-cell transcriptomics uncovers distinct molecular signatures of stem cells in chronic myeloid leukemia. *Nat Med* 2017;**23**:692–702.
32. Vellinga TT, Borovski T, de Boer VC, Fatrai S, van Schelven S, Trumpi K, Verheem A, Snoeren N, Emmink BL, Koster J, et al. SIRT1/PGC1alpha-dependent increase in oxidative phosphorylation supports chemotherapy resistance of colon cancer. *Clin Cancer Res: Off J Am Assoc Cancer Res* 2015;**21**:2870–9.
33. Sharma SV, Lee DY, Li B, Quinlan MP, Takahashi F, Maheswaran S, McDermott U, Azizian N, Zou L, Fischbach MA, et al. A chromatin-mediated reversible drug-tolerant state in cancer cell subpopulations. *Cell* 2010;**141**:69–80.
34. Sancho P, Burgos-Ramos E, Tavera A, Bou Kheir T, Jagust P, Schoenhals M, Barneda D, Sellers K, Campos-Olivas R, Grana O, et al. MYC/PGC-1alpha balance determines the metabolic phenotype and plasticity of pancreatic cancer stem cells. *Cell Metab* 2015;**22**:590–605.
35. Corominas-Faja B, Oliveras-Ferreros C, Cuyas E, Segura-Carretero A, Joven J, Martin-Castillo B, Barrajon-Catalan E, Micol V, Bosch-Barrera J, Menendez JA. Stem cell-like ALDH(bright) cellular states in EGFR-mutant non-small cell lung cancer: a novel mechanism of acquired resistance to erlotinib targetable with the natural polyphenol silibinin. *Cell Cycle* 2013;**12**:3390–404.
36. Lain S, Hollick JJ, Campbell J, Staples OD, Higgins M, Aoubala M, McCarthy V, Appleyard V, Murray KE, Baker L, et al. Discovery, in vivo activity, and mechanism of action of a small-molecule p53 activator. *Cancer Cell* 2008;**13**:454–63.